



Cite this: *Environ. Sci.: Nano*, 2026, 13, 2135

## Sustainable production of selenium-rich and cadmium-safe rice by nZVI–melatonin synergy via coordinated plant–microbe regulation

Saiqa Menhas,<sup>abc</sup> Minjie Chen,<sup>ac</sup> Hui Jin,<sup>ac</sup> Jiang Xu,<sup>ac</sup> Saiyong Zhu,<sup>id b</sup> Muhammad Iqbal Zaman,<sup>d</sup> Jie Hou<sup>id \*ac</sup> and Daohui Lin<sup>id abc</sup>

Developing environmental regulation strategies to reduce cadmium (Cd) accumulation in rice while promoting selenium (Se) enrichment is crucial for global food safety and remains a significant challenge. Here, we evaluated a stage-specific co-application approach involving nanoscale zero-valent iron (nZVI) amendment to soil and foliar spraying of melatonin (MT), which decreased grain Cd concentrations by up to 64% while elevating grain Se content by up to 74% in pot experiments. It also enhanced the Se bioconcentration factor ( $\approx 63\%$ ) and the leaf-to-grain translocation factor ( $\approx 77\%$ ), indicating improved uptake and redistribution under Cd stress. Mechanistic analyses revealed synergistic metabolic reprogramming: antioxidant defenses were strengthened by elevated ascorbate peroxidase activity, which reduced hydrogen peroxide and restored redox homeostasis. Transcriptomic profiling revealed suppression of Cd influx transporters and activation of genes involved in vacuolar sequestration, antioxidant metabolism, and Se transport, thereby restricting Cd translocation while promoting Se accumulation. Rhizosphere microbiomes were enriched with beneficial taxa, including *Pseudomonadota*, *Acidobacteriota*, and *Bacillota*, which contributed to Cd stabilization and Se bioavailability. This nZVI–MT combined strategy offers a viable strategy for producing safe and nutritious rice.

Received 18th October 2025,  
Accepted 13th March 2026

DOI: 10.1039/d5en00966a

rsc.li/es-nano

### Environmental significance

Achieving Cd detoxification and Se biofortification in rice grown on Cd-contaminated soils is a critical but unresolved challenge. This study demonstrates that co-application of nanoscale zero-valent iron (nZVI) and melatonin (MT) at the tillering stage reduced grain Cd by up to 64% while enhancing Se by up to 74% in pot experiments. The combined treatment also increased Se bioconcentration and leaf-to-grain translocation, reflecting improved uptake and redistribution. Mechanistic evidence indicated suppressed Cd influx, enhanced vacuolar sequestration, upregulated Se transporters, and enriched beneficial microbial taxa, collectively enabling dual outcomes. This approach provides a viable strategy for safe and nutritious rice production.

## 1. Introduction

Rice (*Oryza sativa*) is a primary staple for more than half of the global population, but its quality and nutritional value are increasingly threatened by cadmium (Cd) contamination in paddy soils.<sup>1,2</sup> In affected rice-growing regions, soil Cd concentrations can range from 0.1 to 42.9 mg kg<sup>-1</sup>, posing serious health risks, including carcinogenicity and

nephrotoxicity, as well as cardiovascular and neurological disorders, underscoring the need to minimize Cd accumulation in rice. Concurrently, selenium (Se), an essential micronutrient integral to antioxidant enzyme systems, confers significant protection against chronic and infectious diseases.<sup>3</sup> While Se-biofortified rice enhances both nutritional and economic value, an estimated 0.5–1 billion individuals worldwide suffer from Se deficiency due to inherently low soil Se bioavailability.<sup>4</sup> In China, some Se-rich regions face the dual problem of Se enrichment and Cd co-contamination, with 24–56% of Se-rich rice exceeding the Cd safety limit of 0.2 mg kg<sup>-1</sup>.<sup>5</sup> Cd and Se frequently co-occur in paddy soils, especially near mining areas, and show positively correlated accumulation in rice due to co-enrichment in soil deposits and weathering products.<sup>6</sup> Selectively reducing Cd while promoting Se uptake is therefore a key agricultural challenge, complicated by the fact that their bioavailability

<sup>a</sup> State Key Laboratory of Soil Pollution Control and Safety, College of Environmental and Resource Sciences, Zhejiang University, Hangzhou 310058, China. E-mail: hou-jie@zju.edu.cn

<sup>b</sup> Zhejiang Ecological Civilization Academy, Anji 313300, P. R. China

<sup>c</sup> Zhejiang Provincial Key Laboratory of Organic Pollution Process and Control, College of Environmental and Resource Sciences, Zhejiang University, Hangzhou 310058, P. R. China

<sup>d</sup> Department of Chemistry, University of Science and Technology, Bannu 28100, KP, Pakistan



and mobility in plants vary across growth stages, affecting redox homeostasis and defense signaling.

Nanotechnology offers promising tools for heavy metal management in agriculture.<sup>7–10</sup> Nanoscale zero-valent iron (nZVI) is among the most effective amendments for reducing soil Cd bioavailability through adsorption, co-precipitation, and redox transformation.<sup>11</sup> In flooded soils, nZVI oxidizes rapidly to magnetite and goethite, which bind labile Cd and promote iron plaque formation on root surfaces, creating a physical barrier to Cd entry.<sup>5,12,13</sup> Molecular studies have shown that nZVI modulates Cd transporters (*OsZIP*, *OsNRAMP*, and *OsHMA*), enhances Cd tolerance (via *OsCDT* and *OsMTP*), and influences the transcription of vacuolar sequestration genes (*OsPCS*, *OsLCT*, *OsABCC*, and *OsMT*), resulting in more than 50% inhibition of Cd translocation to grains in certain instances.<sup>13–15</sup> However, nZVI strongly sorbs selenite ( $\text{SeO}_3^{2-}$ ), potentially reducing Se bioavailability by 20–40% under conditions favorable for Fe oxide complexation.<sup>5,11,16–21</sup> This inherent trade-off between Cd detoxification and Se biofortification necessitates complementary approaches.

Melatonin (MT) is a potent redox regulator and plant growth promoter that can enhance Se uptake while reducing Cd accumulation.<sup>22–26</sup> Foliar MT application can boost Se content by improving antioxidant capacity, modulating nutrient transport, and regulating stress responses.<sup>25</sup> Under Cd stress, MT enhances root vigor, chlorophyll content, and photosynthetic efficiency, while reducing oxidative damage indicators including hydrogen peroxide and malondialdehyde.<sup>27,28</sup> It also promotes glutathione and phytochelatin synthesis for vacuolar Cd sequestration, limits Cd mobility, and improves grain Se by enhancing root uptake and translocation.<sup>24,29</sup> Se supplementation and MT biosynthesis interact synergistically, activating antioxidant enzymes and alleviating Cd toxicity.<sup>23,30</sup> MT also modulates phosphorus, sulfate, and silicon transporters, supporting Se uptake and maintaining Fe homeostasis under Cd stress.<sup>31–34</sup> Evidence further suggests that combining MT with nanomaterials such as zinc oxide nanoparticles or nZVI can yield synergistic benefits, reducing Cd concentration while enhancing micronutrient enrichment.<sup>11,35,36</sup> Therefore, further exploration of the detailed biochemical and molecular mechanisms involved is warranted.

Here, we hypothesize that co-application of nZVI to soil and MT to foliage can synergistically reduce Cd uptake and translocation to rice grains while enhancing Se enrichment in grains, through coordinated regulation of ion transport, antioxidant defense, and the rhizosphere microbial community. To test this hypothesis, we conducted pot experiments using a rice cultivar (*O. sativa* L. subsp. *japonica* Kato) grown in Cd-contaminated paddy soils. Treatments included single and combined applications of nZVI (soil) and MT (foliar) at specific growth stages, with systematic evaluation of plant growth and yields, grain and tissue Cd and Se contents, oxidative stress and antioxidant responses, transcriptomic profiles, and microbial community dynamics.

The results are expected to elucidate how nZVI–MT synergy reprograms plant and microbial pathways to enable selective Cd detoxification and Se biofortification, providing mechanistic insights into a sustainable strategy for producing safer, nutrient-rich rice in heavy metal-contaminated agroecosystems.

## 2. Materials and methods

### 2.1. Sample collection and soil preparation

The conventional japonica rice cultivar Jia58 was selected for this study. MT (purity >98%) and all analytical-grade reagents were purchased from Aladdin Chemical Reagent Company (Shanghai, China). Commercial nZVI (average particle size ~100 nm) was obtained from Guangzhou Hongwu New Material Technology Co., China. Contaminated paddy soil was collected from a field in northwestern Zhejiang Province, historically affected by coal mining tailings. The air-dried soil was passed through a 2 mm sieve, with a texture of 18% silt, 62% sand, and 19% clay. Previous studies<sup>7,37,38</sup> reported enrichment of both Cd and Se at this site, with mean background levels of 23.21 mg kg<sup>-1</sup> for Cd and 3.73 mg kg<sup>-1</sup> for Se, exceeding Chinese agricultural thresholds (>0.6 mg kg<sup>-1</sup> for Cd and >0.4 mg kg<sup>-1</sup> for Se).<sup>21</sup> The key physicochemical properties of the soil and nZVI, along with the initial background concentrations of Cd and Se, are presented in Table S1 and Fig. S1 (Appendix A). The data reported in this study correspond to post-harvest soil Cd and Se measurements.

For nZVI treatments, a subsample of soil was amended at 100 mg kg<sup>-1</sup> and homogenized by shaking at 180 rpm for 2 h at 25 °C.<sup>7,8</sup> The amended soil was then blended with the remaining bulk soil for each pot and further mixed for 2 h to ensure uniform dispersion.<sup>39</sup> Soils were pre-incubated for one week to stabilize amendment reactions prior to planting. The selected dose of 100 mg kg<sup>-1</sup> (equivalent to 200 mg nZVI pot<sup>-1</sup>) was based on our previous experimental findings,<sup>7,8</sup> which demonstrated that an application rate of 100 mg kg<sup>-1</sup> nZVI effectively reduced Cd accumulation in rice, thereby supporting both comparability across studies and the efficacy of Cd immobilization in the current investigation.

### 2.2. Experimental design

Rice seeds were sterilized with 10% hydrogen peroxide ( $\text{H}_2\text{O}_2$ ) for 15 min and rinsed three times with ultrapure water. The seeds were then germinated in a growth chamber under controlled conditions: 14 hour (h) light and 10 h dark, 25 ± 5 °C, 300–500 μmol m<sup>-2</sup> s<sup>-1</sup> light intensity, and 70–80% relative humidity. After 28 days (d) of initial growth, two uniform rice seedlings were transplanted into individual polyethylene pots containing 2 kg of either untreated or nZVI-amended soil. A one-week acclimation period was provided to allow the plants to stabilize under the new growth conditions. Subsequently, MT was applied as a foliar spray at a concentration of 200 μM, with a total volume of 30 mL (approximately 1.4 mg of MT) per pot per day.<sup>38</sup> The spray was evenly distributed over both the adaxial and abaxial



leaf surfaces. This treatment was administered once daily for seven consecutive days during two critical growth stages: tillering (T) and flowering (F). The T stage commenced one week after transplantation, while the F stage began approximately two months after transplantation (~80 days after sowing). MT application at the T stage in combination with nZVI delayed flowering, whereas MT application alone resulted in the earliest flowering, indicating treatment-specific effects on developmental timing. The concentration of 200  $\mu\text{M}$  melatonin was selected based on established evidence from our previous work,<sup>38</sup> demonstrating its effectiveness in enhancing Cd detoxification, activating plant defense systems, and improving stress tolerance. Untreated plants in Cd-contaminated soil (TF-Cd) served as controls. The experimental design included MT and/or nZVI treatments at both stages to assess their temporal effects. The MT (200  $\mu\text{M}$ ) and nZVI (100  $\text{mg kg}^{-1}$ ) concentrations were selected based on prior validation and preliminary studies,<sup>7,8,38</sup> demonstrating optimal, non-toxic, and synergistic mitigation of Cd stress.

The experiment employed a completely randomized design with six treatment groups, each with four biological replicates ( $n = 4$ ), yielding a total of 24 experimental pots. Treatments were structured to evaluate the individual and stage-specific combinatorial effects of nZVI (100  $\text{mg kg}^{-1}$  soil-applied) and MT (200  $\mu\text{M}$  foliar-applied) under Cd stress, as follows: (1) TF-Cd: Cd-exposed control (no nZVI or MT); (2) TF-Cd + nZVI: soil treated with 100  $\text{mg kg}^{-1}$  nZVI; (3) T-Cd + MT: 200  $\mu\text{M}$  MT applied only at the T stage; (4) F-Cd + MT: 200  $\mu\text{M}$  MT applied only at the F stage; (5) T-Cd + MT + nZVI: 100  $\text{mg kg}^{-1}$  nZVI + 200  $\mu\text{M}$  MT (at the T stage); (6) F-Cd + MT + nZVI: 100  $\text{mg kg}^{-1}$  nZVI + 200  $\mu\text{M}$  MT (at the F stage). The label 'TF' refers to treatment groups that did not receive stage-specific MT application, and thus serve as baseline controls. These groups enable us to assess and isolate the specific effects of MT application during the T and F stages, both in the presence and absence of nZVI amendment. All treatments were performed in a glasshouse at Zhejiang Ecological Civilization Academy (Huzhou City, China). The environmental conditions were maintained at 25  $^{\circ}\text{C}$ , 70–75% relative humidity, a 14 h light and 10 h dark cycle, and a light intensity of 300–500  $\mu\text{mol m}^{-2} \text{s}^{-1}$ . Water was replenished daily to maintain a  $2.0 \pm 1.0$  cm water layer above the soil surface. Fertilizer was applied once at the 60th d after sowing, including 30  $\text{mg kg}^{-1}$  nitrogen ( $\text{NH}_4\text{NO}_3$ ), 30  $\text{mg kg}^{-1}$  potassium ( $\text{KNO}_3$ ), and 10  $\text{mg kg}^{-1}$  phosphorus ( $\text{KH}_2\text{PO}_4$ ). Plants were harvested 140 d after sowing (112 days after transplantation; DAT) to assess growth, yields and physiological and biochemical traits. Tissues were either used fresh, stored at  $-80$   $^{\circ}\text{C}$ , or oven-dried at 68  $^{\circ}\text{C}$  for 48 h until constant weight.

### 2.3. Evaluation of plant growth and grain yields

Plants were carefully washed with tap water followed by ultrapure water 3 times. Shoot length and root length were

measured using a ruler. Fresh weight and dry weight were recorded using an electronic balance (Sartorius BSA623S).<sup>38</sup> The number of panicles was recorded per pot, and the grain yield was determined with and without husk.

### 2.4. Estimation of stress biomarkers and antioxidant activities

Following the final MT application at the F stage, leaf samples were collected (90 DAT) for estimation of stress biomarkers and antioxidant activities. For each replicate, 0.1 g fresh flag leaf tissue was homogenized in 2 mL ice-cold phosphate buffer (0.1 M, pH 7.4) and centrifuged at 12 000g for 20 min at 4  $^{\circ}\text{C}$ . The supernatant was used for further biochemical assays.<sup>40</sup>  $\text{H}_2\text{O}_2$ , malondialdehyde (MDA), proline (Pro), and total soluble protein (TSP) were determined using assay kits (A064-1-1, A003-3-1, A107-1-1, and A045-2-2, respectively) from Nanjing Jiancheng Bioengineering Institute, China. TSP was quantified by the Coomassie brilliant blue method and expressed as g protein per L. Antioxidant enzymes, including superoxide dismutase (SOD), peroxidase (POD), catalase (CAT), ascorbate peroxidase (APX), and glutathione reductase (GR) were measured using corresponding kits (A001-1, A084-3-1, A007-1-1, A123-1-1, and A062-1, respectively), with results reported as U  $\text{g}^{-1}$  FW or U  $\text{mg}^{-1}$  protein, depending on the assay.

### 2.5. Determination of Cd and Se in soil and plant samples

For metal quantification, 0.2 g of dried plant tissue (shoots, roots, and grains) was digested with 10 mL concentrated  $\text{HNO}_3$  and 5 mL  $\text{H}_2\text{O}_2$  using a microwave digestion system (MARS6, CEM, USA). Soil samples (0.2 g) were digested with a mixed acid solution ( $\text{HCl}$ ,  $\text{HNO}_3$ , HF, and  $\text{HClO}_4$ ) as previously described.<sup>7,8,38</sup> Cd and Se concentrations were determined using inductively coupled plasma mass spectrometry (ICP-MS, Optima 8000, PerkinElmer, USA). Standard reference materials (GBW10045a for rice and GBW07401a for soil) were used to ensure analytical accuracy. The bioaccumulation coefficient (BAC), bioconcentration factor (BCF), and translocation factor (TF) were calculated. The BAC is defined as the ratio of tissue to soil metal concentrations, the BCF as the grain-to-soil ratio, and the TF as the grain-to-leaf ratio.<sup>40,41</sup>

### 2.6. RNA sequencing and transcriptomic analysis

Following the final MT application at the F stage, leaf samples in each group were collected (75 DAT) from the plant and rinsed. Total RNA of the samples was extracted using an EasyPure® plant RNA kit (ER301-01, TransGen Biotech). The quality of RNA was assessed using 1% agarose gel, a 2100 bioanalyzer (Agilent Technologies), and a NanoDrop2000 spectrophotometer (Thermo Fisher Scientific, USA). The quantified RNA was used to construct the sequencing library and sequenced by Shanghai Majorbio Bio-pharm Biotechnology Co., Ltd. (Shanghai, China). Raw reads were filtered using FASTP (<https://github.com/OpenGene/fastp>)



while HISAT2 (<https://ccb.jhu.edu/software/hisat2/index.shtml>) was used to map the clean reads to the reference genome. StringTie (<https://ccb.jhu.edu/software/stringtie/>) was used to assemble the mapped reads for each sample. The RNA-seq experiments were replicated 3 times for each treatment. Gene expression levels were quantified using the transcripts per million reads method and analyzed for differentially expressed genes (DEGs) using DESeq2/DEGseq/edgeR/Limma/NOIseq tools ( $P\text{-adjust} \leq 0.05$ ,  $|\log_2(\text{fold change})| \geq 1$ ). Gene Ontology (GO) (<https://github.com/tanghaibao/Goatools>) and Kyoto Encyclopedia of Genes and Genomes (KEGG) (<https://kobas.cbi.pku.edu.cn/home.do>) enrichment analyses were performed to elucidate the most important biochemical function terms and metabolic pathways associated with the DEGs, respectively.

### 2.7. Soil microbial diversity analysis

The rhizosphere soil samples from mature rice roots in TF-Cd (control), TF-Cd + nZVI (nZVI treatment), and T-Cd + MT + nZVI (MT application at the T stage combined with nZVI) were used (112 DAT) to evaluate the effect of nZVI alone and combined with MT at the T stage on soil microbial communities. Soil microbiome analysis was limited to T-stage treatments, as this stage exhibited the most pronounced responses and directly aligned with the study's objective of evaluating stage-specific MT-nZVI synergistic effects; therefore, the F-Cd + MT + nZVI treatment was excluded. Homogenized soil samples were stored at  $-80^\circ\text{C}$  prior to DNA extraction. About 0.5 g of soil from each biological replicate was used for DNA extraction using a soil DNA isolation kit (MOBIO, USA). The concentration and purity of DNA (OD260/OD280 and OD260/OD230) after extraction were determined with an ultra-micro ultraviolet spectrophotometer (Nanodrop X210, America). The V3-V4 hypervariable regions of bacterial 16 S rRNA genes were amplified using the primers 338 F (5'-ACTCCTACGGGAGGCA GCAG-3') and 806 R (5'-GGACTACHVGGGTWTCTAAT-3'). Principal coordinate analysis (PCoA) was run to compare the microbial community structures across all soil samples.

### 2.8. Quality control and statistical analysis

All results were subjected to quality assurance procedures, utilizing standard solutions from Merck. Standard reference materials (rice GBW10045a and soil GBW07401a) were employed for quality control during elemental analyses. Data from treated and control plants ( $n = 4$ ) were statistically analyzed using the Statistical Package for the Social Sciences (SPSS) software version 23.0 (Chicago, IL, USA). Analysis of variance (ANOVA), followed by Duncan's multiple range test (DMRT), was performed to identify significant differences between the mean values ( $n = 4$ ;  $p < 0.05$ ). For each treatment, the RNA-Seq assay and 16 S rRNA seq were repeated three times. Graphs were generated using Origin software version 9.1 (Origin Lab, Berkeley, CA, USA) and Majorbio Cloud (<https://www.majorbio.com/>).

## 3. Results and discussion

### 3.1. Stage-dependent synergy of nZVI and MT in mitigating Cd stress and promoting Se enrichment in rice

Cd contamination impairs rice growth, with stage-dependent effects driven by shifting physiological priorities: during the T stage, the plant prioritizes vegetative expansion and photosynthetic capacity building (source development), whereas during the F stage, resources are redirected toward reproductive structure formation and grain filling (sink dominance).<sup>3,11,42-44</sup> To capture these stage-specific responses, we evaluated the effects of MT, nZVI, and their combined application at the T and F stages. From the perspective of overall appearance, no obvious visual differences were observed among the treatment groups (Fig. 1a and b); however, the fresh weights of root and shoot tissues as well as rice grain yields exhibited clear variations. At the T stage, foliar MT treatment alone (T-Cd + MT) increased the root length and shoot length by 19.4% and 5.5% (both  $p < 0.05$  versus the TF-Cd control), while the addition of nZVI (T-Cd + MT + nZVI) further improved the shoot length by 3.4% ( $p < 0.05$ ). Biomass peaked under the T-stage combined treatment, with root and shoot fresh weights increasing by 53.4% and 35.3%, respectively (both  $p < 0.05$ ) (Fig. 1c). Yield responses showed stage dependence: F-Cd + MT achieved the greatest increases, raising the grain yield with husk by 32.8% and without husk by 38.5% (both  $p < 0.05$ ), whereas T-Cd + MT improved the husked yield by 19.95% ( $p < 0.05$ ). Both MT and nZVI single treatments reduced the panicle number, with a 22.1% decrease under F-Cd + MT ( $p < 0.05$ ). The higher grain yield despite the lower panicle number in F-Cd + MT likely reflects MT's stronger effect on grain filling, mediated by improved elemental regulation and redox homeostasis, rather than on panicle initiation. Moreover, this phenomenon can be attributed to the fact that both nZVI and MT exert concentration-dependent effects on plants, characterized by growth stimulation at low concentrations but inhibition at elevated levels, *e.g.*, the threshold for MT-induced growth inhibition can be as low as  $100\ \mu\text{M}$ ,<sup>45,46</sup> whereas growth suppression by nZVI typically occurs only at approaching  $1000\ \text{mg}\ \text{kg}^{-1}$ .<sup>39</sup> Importantly, our research first reported that nZVI-MT co-application maintained or slightly increased the panicle number (Fig. 1d and e), highlighting the synergistic benefit of MT and nZVI co-application in sustaining higher rice yields.

Cd and Se partitioning provided mechanistic explanations for these stage-dependent effects. Compared with the TF-Cd control, nZVI alone reduced Cd by 33.3% in roots, 55.0% in leaves, and 64.3% in grains, achieving the lowest grain Cd bioconcentration factor (BCF) ( $p < 0.05$ ) (Fig. 2a and b and S2, Appendix A). The T-stage co-application of nZVI and MT produced comparable Cd reductions, 34.6% in roots, 65.2% in stems, 67.6% in leaves, and 52.1% in grains, with a 41.9% decrease in grain Cd BCF (all  $p < 0.05$ ), while avoiding yield penalties. The Cd translocation factor from leaves to grains



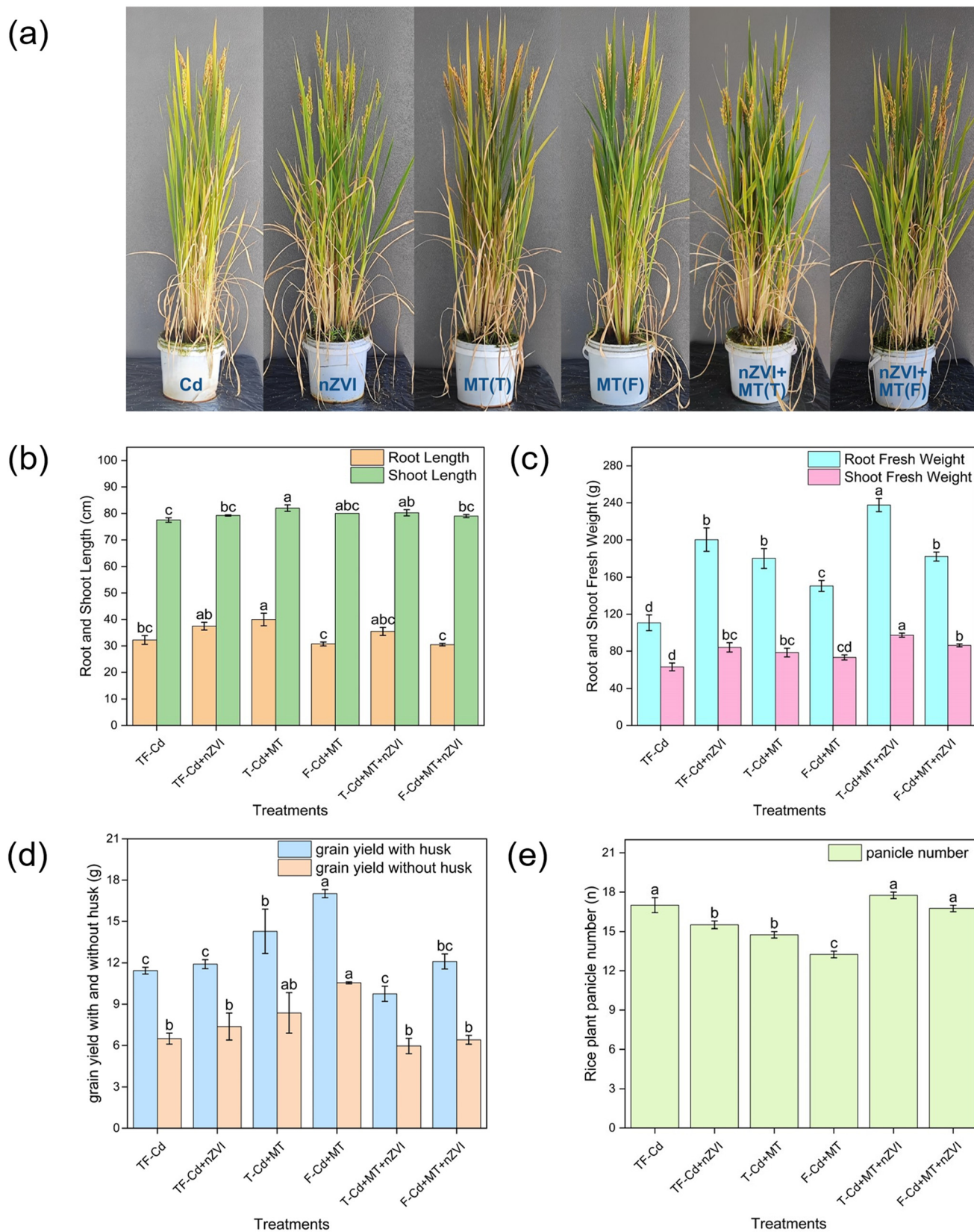


**Fig. 1** Effects of nZVI and MT on rice growth and productivity at the T and F stages. (a) Plant morphology; (b) root and shoot lengths; (c) root and shoot fresh weights; (d) grain yield with husk and without husk; (e) panicle number. Bars annotated with different superscript letters indicate significant differences among treatments ( $p < 0.05$ ).



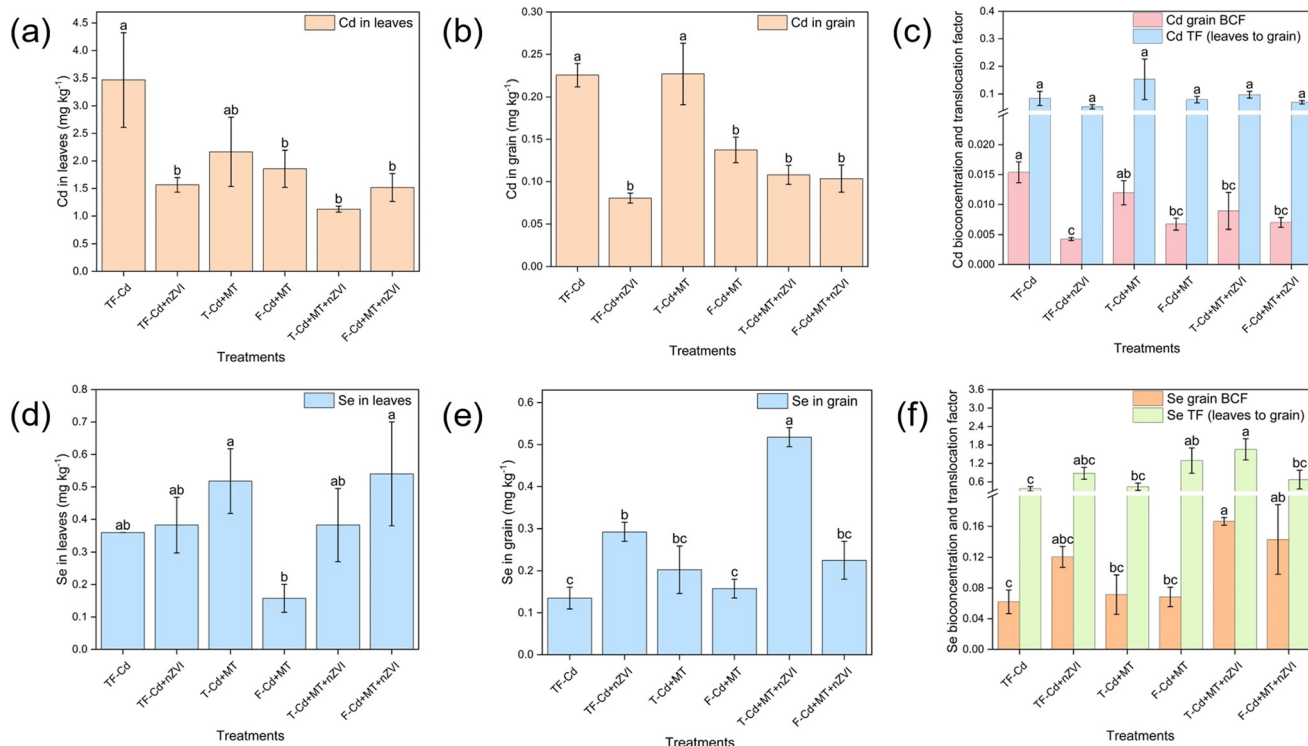


**Fig. 2** Effects of nZVI and MT on the Cd accumulation in (a) leaves and (b) grains, (c) the Cd grain bioconcentration and translocation factor, the Se accumulation in (d) leaves and (e) grains, and (f) the Se grain bioconcentration and translocation factor. All the means sharing different letters significantly differ at the  $p < 0.05$  level.

remained unchanged, suggesting restriction at uptake and long-distance transport (Fig. 2c). In the soil, Cd availability showed only nonsignificant shifts across treatments, supporting that observed changes mainly arose from plant-level processes (Fig. S2). In contrast, Se dynamics revealed clear advantages of the combined treatment (Fig. 2 and S3). Although Se in the leaves exhibited no significance between the control and treatment groups (Fig. 2d), grain Se increased by 73.9% under T-Cd + MT + nZVI (Fig. 2e), compared with 53.8% under nZVI alone and 56.6% under F-Cd + MT + nZVI, with the highest Se translocation factor (77.4%) occurring at the T stage (Fig. 2f). Given that selenite strongly adsorbs onto iron (hydr)oxides,<sup>5</sup> the single application of Fe-based materials such as iron monosulfide (100 mg L<sup>-1</sup>) reduced Cd accumulation in grains while concurrently diminishing Se uptake. Numerous studies demonstrate the efficacy of nanomaterials in mitigating both Se and Cd contamination.<sup>11,16–19</sup> For example, 1.3 mM selenite was completely removed within 3 min using 5 g L<sup>-1</sup> nZVI.<sup>16</sup> Similarly, biochar-ZVI exhibited high sorption capacities for Se(IV) (62.52 mg g<sup>-1</sup>) and Se(VI) (35.39 mg g<sup>-1</sup>),<sup>47</sup> while FeO-NPs and Se-NPs (15–30 mg L<sup>-1</sup>) alleviated Cd toxicity in plants grown in soils with 50 mg kg<sup>-1</sup> Cd.<sup>17</sup> Furthermore, 100 mg L<sup>-1</sup> FeS removed 93.2% of Se(IV) through reduction to Se(0), concomitant with the oxidation of FeS to goethite (78.9%), lepidocrocite (21.1%), and elemental sulfur (91.5%), as confirmed by X-ray absorption fine structure (XAFS) spectroscopy.<sup>18</sup> In parallel, nZVI has been reported to reduce

grain Cd concentration by >80% in contaminated soils<sup>11</sup> and to remove 20–52% of aqueous Cd (100 μM) at doses of 50–200 mg L<sup>-1</sup>, primarily *via* adsorption and surface complexation. Additionally, nZVI promotes the formation of iron plaque on roots, increasing their biomass by up to 267%, which act as effective barriers against Cd uptake.<sup>19</sup> In contrast, the T-stage nZVI–MT combination in this study preserved the strong Cd-limiting capacity of nZVI while simultaneously improving Se delivery to grains and maintaining biomass and yields. Collectively, this stage-aware framework indicates that F-stage MT is optimal for yield improvement, nZVI alone ensures strong Cd restriction but risks Se loss, and T-stage nZVI–MT co-application uniquely balances both outcomes to achieve high agronomic benefit.

The observed Cd declines in this study are consistent with the established role of nZVI in decreasing the bioavailability of free Cd<sup>2+</sup> species in the rhizosphere, thereby restricting their uptake into rice roots and subsequent translocation *via* the xylem.<sup>13</sup> Concurrently, nZVI at a concentration of 100 mg L<sup>-1</sup> has been shown to alleviate Cd (10 μM) stress in rice by enhancing antioxidant defenses, modulating metal transporter gene expression, reducing Cd uptake/translocation, immobilizing Cd in soil, and improving the grain yield under metal stress.<sup>13</sup> The unchanged translocation factors across treatments further suggest that regulation occurs primarily at the points of uptake and systemic movement rather than during leaf-to-grain partitioning. Under Cd stress, rice is known to enhance high-affinity Cd influx



systems while attenuating detoxification pathways, which normally favors root-to-shoot transfer.<sup>14,48,49</sup> By counteracting these responses, nZVI can effectively suppress Cd flux within the plant. For Se, prior studies highlight a frequent trade-off, where nZVI strongly restricts Cd but can decrease Se uptake by ~20–40% due to selenite interactions with Fe oxides, even as it strongly lowers grain Cd by >50–85%.<sup>5,20,21</sup> Our present findings demonstrate a way to circumvent this limitation. When combined with MT at the appropriate developmental stage, the system retained the Cd-limiting benefits of nZVI while simultaneously enhancing Se allocation to grains. This outcome highlights a shift from the conventional “Cd–Se trade-off” paradigm. MT likely strengthens antioxidant capacity, engages phosphate and sulfur transporter networks, and thus facilitates Se mobilization and long-distance translocation.<sup>11,17,50,51</sup> Overall, this stage-dependent synergy underscores an agronomic strategy by aligning the physiological timing of MT with the Cd-restricting function of nZVI to achieve a dual goal of Cd mitigation and Se biofortification.

### 3.2. Redox homeostasis modulation by nZVI–MT lowers ROS burden and attenuates Cd toxicity

Across both T and F stages, Cd elevated ROS and lipid peroxidation, whereas the treatments rebalanced the redox

status in distinct ways. nZVI alone lowered H<sub>2</sub>O<sub>2</sub> and MDA by 76.4% and 36.4%, respectively ( $p < 0.05$  vs. Cd control) (Fig. 3a). MT-containing treatments produced the largest H<sub>2</sub>O<sub>2</sub> decreases, with F-Cd + MT, T-Cd + MT, T-Cd + MT + nZVI, and F-Cd + MT + nZVI reducing H<sub>2</sub>O<sub>2</sub> by 95.2%, 94.5%, 92.7%, and 89.2%, respectively (all  $p < 0.05$ ). Total protein increased under every treatment (by 92.6% for F-Cd + MT), and proline rose at the T stage with MT and nZVI + MT (by 31.35% and 32.6%, respectively) (Fig. 3b). At the enzyme level (Fig. 3c and d), the nZVI + MT treatment reduced SOD activity at the T and F stages by 59.9% and 58.1%, respectively, while APX rose with MT-containing treatments (59.0% by F-Cd + MT + nZVI and 40.7% by T-Cd + MT + nZVI). GR decreased under the combined treatments (58.0% at the F stage and 43.2% at the T stage), and CAT and POD were largely unchanged ( $p > 0.05$ ).

These patterns map onto a coherent ROS-network model with H<sub>2</sub>O<sub>2</sub> as the central node (Fig. 3e). First, nZVI acts upstream by limiting Cd entry at the root interface, which suppresses superoxide generation and the need for high SOD throughput; the observed drop in SOD and MDA with nZVI is consistent with “source control” of ROS formation *via* Fe (hydr)oxide-mediated Cd interception.<sup>12,13,52</sup> Because less superoxide is formed, the glutathione cycle is under lower flux demand, which explains the reduced GR despite lower H<sub>2</sub>O<sub>2</sub> and unchanged CAT/POD. Second, MT tunes the detox

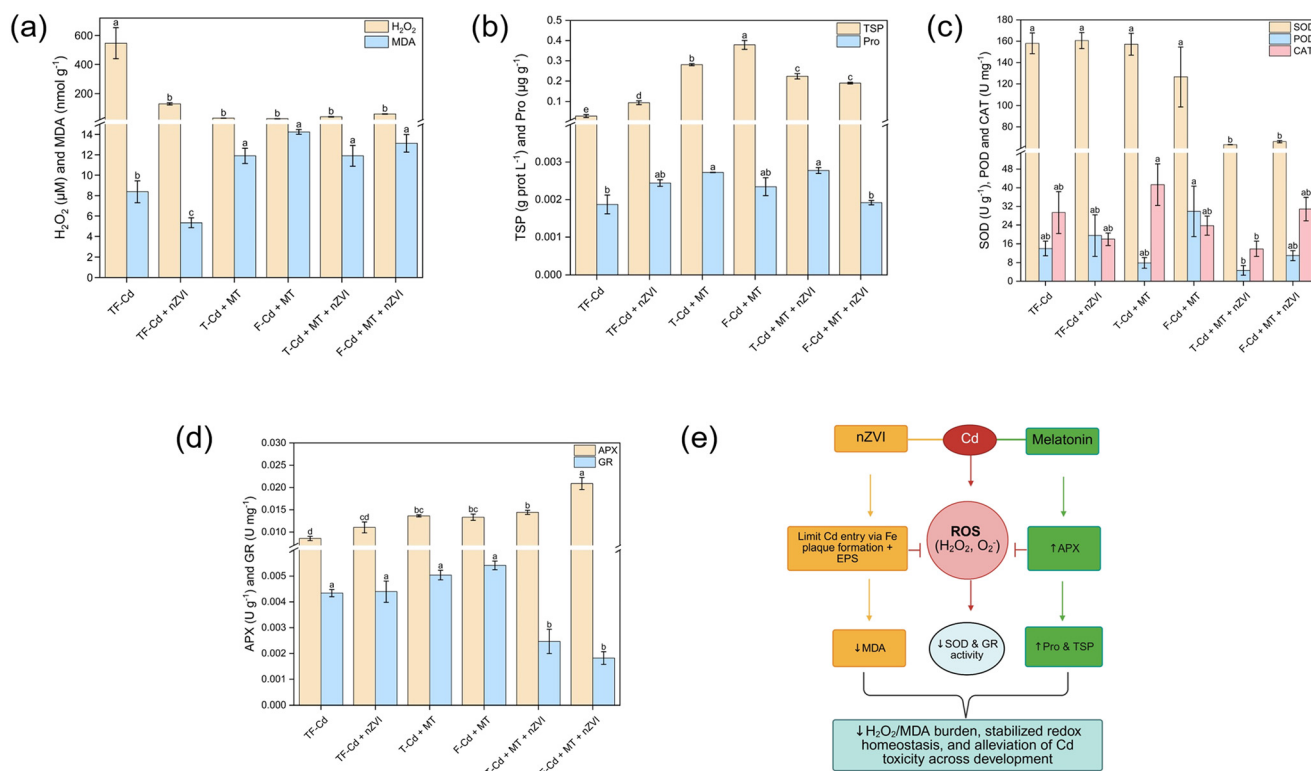


**Fig. 3** Effects of nZVI and MT on redox homeostasis at the T and F stages. (a) H<sub>2</sub>O<sub>2</sub> and malondialdehyde (MDA); (b) proline (Pro) and total soluble protein (TSP); (c) antioxidant enzymes: superoxide dismutase (SOD), peroxidase (POD), and catalase (CAT); (d) ascorbate peroxidase (APX) and glutathione reductase (GR); (e) schematic representation of nZVI–MT-mediated antioxidant mechanisms under Cd stress. EPS; exopolysaccharide production. Values with different superscript letters are significantly different ( $p < 0.05$ ).



arm of the network. MT-containing treatments consistently upregulated APX, the key  $H_2O_2$  sink in the ascorbate-glutathione pathway, and increased compatible solutes (proline) and soluble protein, which stabilize membranes and enzymes under stress.<sup>22,53</sup> The large  $H_2O_2$  reductions with MT or nZVI + MT therefore reflect both diminished ROS

input (nZVI) and enhanced  $H_2O_2$  clearance (MT-driven APX). The modest rise in MDA with MT at both stages (29.6% to 41.2%) likely represents a controlled peroxidation signal associated with remodeling and nutrient redistribution rather than uncompensated damage, as yields were maintained or improved.<sup>28,54</sup>

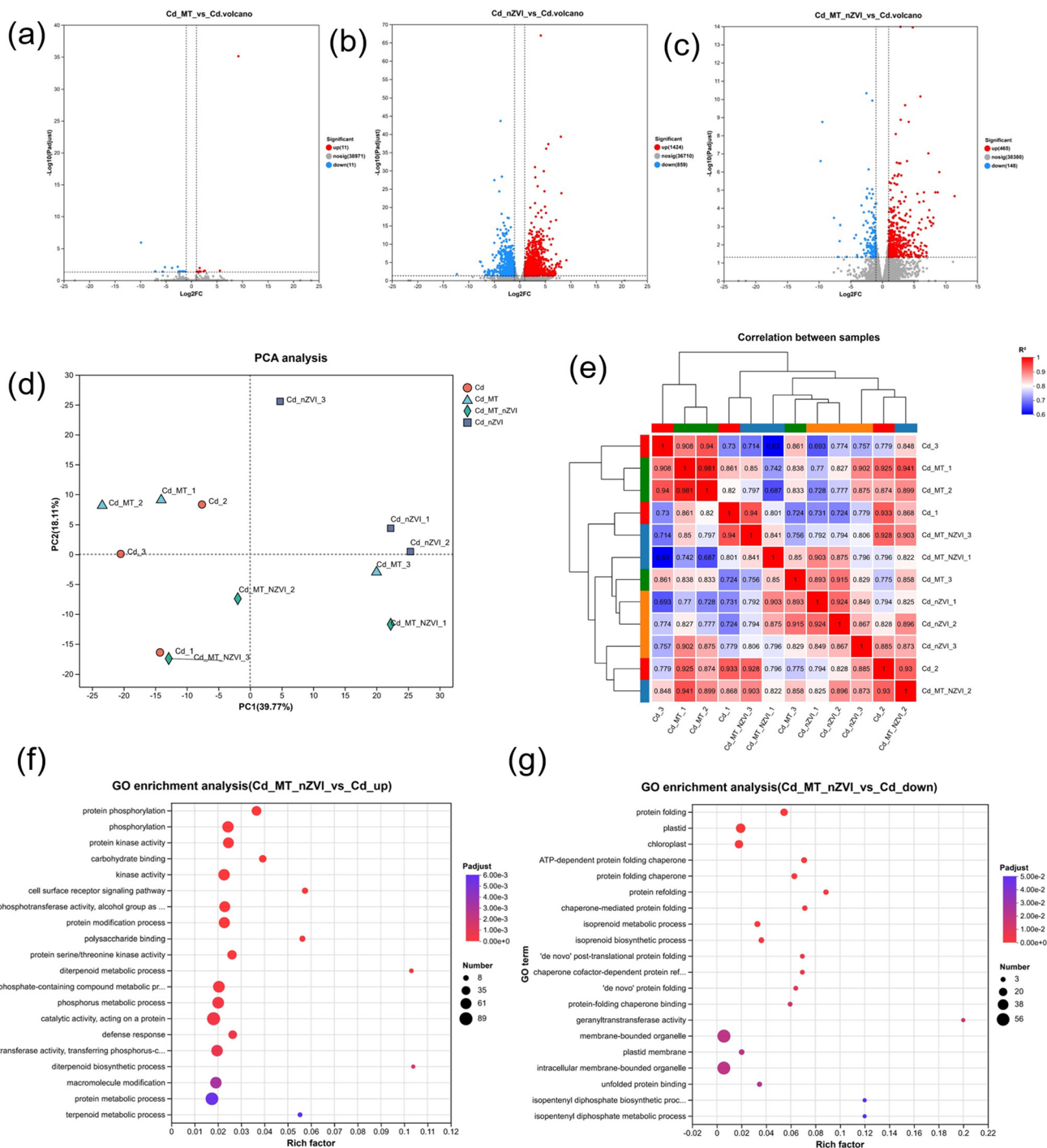


**Fig. 4** Transcriptomic effects of nZVI and MT at the T stage. (a–c) Volcano plots of differentially expressed genes (DEGs) for three comparisons: Cd + MT vs. Cd, Cd + nZVI vs. Cd, and Cd + MT + nZVI vs. Cd; (d) principal component analysis (PCA); (e) correlation matrix; (f) upregulated and (g) downregulated gene ontology (GO) terms in the Cd vs. Cd + MT + nZVI comparison. “Cd” = TF-Cd (Cd-only control); “Cd + MT” = T-Cd + MT (MT applied at the T stage); “Cd + MT + nZVI” = T-Cd + MT + nZVI (MT at the T stage + nZVI soil amendment).



Stage specificity further clarifies roles. At the T stage, nZVI + MT produced strong H<sub>2</sub>O<sub>2</sub> suppression while lowering SOD and GR and elevating APX, together with higher proline and protein, indicating a low-ROS steady state sustained by upstream Cd exclusion plus APX-centered detox. At the F stage, MT's APX stimulation and protein accrual were most pronounced and aligned with the largest yield gains, suggesting effective peroxide control within reproductive sinks.<sup>23,43,55–62</sup> Overall, the data support a division of labor: nZVI curtails ROS generation by restricting Cd flux, and MT reinforces enzymatic and osmotic defenses to clear residual ROS. The net effect is a lower H<sub>2</sub>O<sub>2</sub>/MDA burden, stabilized redox homeostasis, and attenuation of Cd toxicity across development.

### 3.3. Transcriptomic evidence for coupled transport and redox pathways achieving grain Cd restriction and Se enrichment

Transcriptomic profiling further reveals DEGs under nZVI and MT treatments (Tables S1–S3 in Appendix B; Fig. S4 and S5 in Appendix A). Differential expression was minimal with MT alone (22 genes), extensive with nZVI alone (2283 genes), and intermediate with the co-application (613 genes) (Fig. 4a–c), suggesting that the MT combined treatment may alleviate the stress caused by the sole application of nZVI at transcriptional levels. Across nZVI vs. Cd and nZVI + MT vs. Cd, 244 DEGs overlapped; 158 of these (95 up, 63 down) formed the core T stage response (Fig. S6). Clustering and PCA analyses separated the treatment groups with high reproducibility ( $r = 0.8–1.0$ ), indicating clear transcriptional distinctions among treatments and strong consistency across biological replicates (Fig. 4d and e).

GO enrichment provides a mechanistic bridge from transcripts to phenotypes (Fig. 4f and g). In this study, upregulated biological processes included responses to oxidative stress, glutathione metabolism, phenylpropanoid metabolism, secondary-metabolite biosynthesis, and transmembrane transport; molecular functions centered on oxidoreductase, peroxidase, and glutathione transferase activities; cellular components were enriched at the plasma membrane, apoplast/cell wall, peroxisome, and vacuolar membrane. Representative genes mapping to these terms were *CARP/pepA* (glutathione pathway), *OsPAL02* (phenylpropanoid), *GLO6* (peroxisomal glyoxylate cycle), *GPAT* (membrane remodeling), *OsSAUR11* (hormone signaling), and *OsDXS* (cofactor/precursor supply), along with diterpenoid-biosynthesis genes, such as *OsCPS2/4*, *OsKSL10*, *Oscyp71Z6*, and *OsSDR110C-MS2*, indicating enhanced production of specialized metabolites with potential roles in defense and signaling. This GO profile supports enhanced ligand production and vacuolar or apoplastic sequestration that restricts Cd mobility, together with strengthened peroxisomal and glutathione-linked detoxification that lowers the H<sub>2</sub>O<sub>2</sub> accumulation.<sup>40,63,64</sup> For instance, the induction of phenylpropanoid and unique diterpenoid biosynthetic pathways promoted lignin deposition, which likely reinforced

the apoplastic barrier in roots, impeding Cd influx, limiting radial transport, and reducing Cd translocation to aerial tissues. Key contributors to this process include *OsPAL6* and *OsPAL8*, along with GA-biosynthesis genes such as *OsCPS2*, *OsCPS4*, *OsKSL4*, and *OsKSL7*, and multiple members of the cytochrome P450 (CYP) superfamily.<sup>63</sup> Furthermore, 4-hydroxycinnamic acid (4-HCA), synthesized *via OsPAL02* in the phenylpropanoid pathway, was found to enrich metal-tolerant *Pseudomonadales*, suggesting that a lignin biosynthesis intermediate can modulate leaf microbiome composition and promote microbial homeostasis under metal stress.<sup>64</sup> Moreover, MT upregulated the auxin-responsive protein 21 (*SAU21*) gene, implicating auxin signaling in the regulation of growth-defense balance, while activation of the ascorbate–glutathione cycle further enhanced Cd chelation and contributed to H<sub>2</sub>O<sub>2</sub> scavenging, reinforcing redox homeostasis.<sup>40</sup> These molecular responses align with observed physiological outcomes: at the T stage, co-application reduced grain Cd by 52.1% and grain BCF by 41.9% (by 64.3% with nZVI alone), while grain Se increased by 73.9% and soil-to-grain Se transport rose by 62.7%. Downregulated terms clustered in photosynthesis, light-harvesting complex, chlorophyll binding, starch biosynthesis, protein folding/chaperone-mediated folding, and RNA processing. This attenuation indicates a resource shift away from antenna investment, bulk carbon storage, and protein-folding stress toward redox control and defense metabolism, consistent with the observed reductions in H<sub>2</sub>O<sub>2</sub> and the prominence of ascorbate peroxidase activity. These findings resonate with previous reports demonstrating that under conditions of nutrient homeostasis, plants reorient carbon and energy allocation from primary metabolism (*e.g.*, photosynthesis and protein synthesis) toward antioxidant production, resulting in robust growth with reduced physiological stress.<sup>65</sup>

Transcriptomic and GO enrichment analyses jointly indicate that nZVI and MT act on complementary biochemical pathways that together reprogram rice metabolism to limit Cd mobility and enhance Se allocation. nZVI primarily modulates stress perception, antioxidant defenses, and physical/chemical barriers. It triggers early stress signaling and activates oxidoreductase and peroxidase activities that mitigate Cd-induced ROS, while promoting metal-binding proteins and siderophore biosynthesis to chelate Cd and maintain essential ion homeostasis. nZVI also strengthens cell wall and apoplastic barriers through phenylpropanoid metabolism and lignin deposition, and facilitates vacuolar and organelle sequestration of Cd complexes, thereby restricting Cd entry and long-distance transport.<sup>10,66,67</sup> In parallel, the downregulation of high-affinity Cd uptake transporters (*OsNRAMPs*, *OsZIPs*, and *OsHMAs*) reduced root-to-shoot translocation, whereas detoxification and compartmentalization genes, such as *OsPCS*, *OsABCCs*, *OsMTPs*, *OsLCTs*, and *OsMTs*, were upregulated, together minimizing Cd loading into the phloem and restricting its distribution to edible parts (Table S10 in Appendix B). These



actions explain the consistent 50–85% reductions in grain Cd frequently reported for nZVI. By contrast, MT acts as an amplifier of detoxification and developmental regulation. It enhances the ascorbate–glutathione cycle, narrows the transcriptional stress footprint, and drives proline and protein accumulation for osmoprotection.<sup>40,68,69</sup> MT also supports chloroplast performance and energy balance, counteracting the photosynthetic downregulation typically observed under nZVI.<sup>29,70</sup> Moreover, MT promotes hormone and secondary metabolism (e.g., diterpenoid and momilactone biosynthesis), linking stress adaptation with growth and yields. These effects reinforce source–sink relationships and favor the long-distance allocation of nutrients.

The synergy emerges because nZVI acts as a supplement that initiates stress-responsive and Cd-exclusion pathways, while MT amplifies and stabilizes these signals through targeted redox reinforcement and metabolic support. Importantly, co-application enriched transport and membrane terms consistent with phosphate- and sulfur-linked carriers that facilitate Se flux.<sup>50,51,71</sup> At the same time, transcriptomic evidence indicates broad upregulation of *OsSultrs*, *OsPSTs*, *OsNIPs*, *Lsi1/2*, *NRT1*, and *OsAAPs*, suggesting that Se uptake is enhanced by exploiting shared transport systems with sulfate, phosphate, and nitrogen channels (Table S10 in Appendix B). This was further supported by increased ATP availability and Mg<sup>2+</sup>-dependent cofactors generated through enhanced energy metabolism, enabling efficient assimilation of Se into organic forms such as selenocysteine and selenomethionine. Crucially, suppression of vacuolar Se sequestration genes (e.g., *OsSPX-MFS* and *OsVPEs*) reduced Se retention in vegetative tissues and promoted phloem remobilization toward developing grains. Collectively, these results demonstrate that the nZVI–MT co-application does not merely mitigate Cd toxicity but also actively reprograms molecular and physiological networks to favor the uptake and allocation of beneficial micronutrients such as Se. By integrating nanotechnology-based Cd exclusion with MT-enhanced signaling and nutrient translocation, this dual strategy simultaneously reduces grain Cd levels and biofortifies Se, highlighting its promise for sustainable phytomanagement of contaminated agroecosystems.

### 3.4. Rhizosphere microbial reconfiguration under nZVI–MT at the T stage supports Cd restriction and Se enrichment

The co-application of nZVI and MT at the T stage induced significant restructuring of the rice rhizosphere microbiome, contributing mechanistically to reduced Cd accumulation and enhanced Se biofortification. While alpha-diversity indices (Shannon) were comparable, Chao1, ACE, Simpson, and Sobs values were higher in the Cd + nZVI treatment compared to the Cd + nZVI + MT treatment, indicating a modest reduction in taxonomic richness under the combined application (Fig. 5a and S10 in Appendix A). However, this

modest decrease in richness coincided with fewer differentially regulated plant genes, suggesting functional streamlining rather than a loss of ecological resilience, consistent with the selection of a more specialized, metabolically efficient microbial community. PCoA separated communities by treatment, accounting for 89.09% of the variance in abundance and structure (Fig. 5b), underscoring the strong treatment-specific structuring of the rhizobiome.

At the phylum level, Cd stress alone favored the dominance of *Pseudomonadota* and *Actinomycetota*, taxa commonly associated with metal tolerance (Fig. S11 in Appendix A). The addition of nZVI increased the relative abundance of *Acidobacteriota*, *Bacillota*, and *Bacteroidota*, groups linked to nutrient cycling, exopolysaccharide (EPS) production, and iron redox transformations.<sup>7,11,72–77</sup> Notably, *Bacillota* may promote the formation of iron (hydr)oxide plaque on root surfaces, which serve as effective sorption sites for Cd, thereby limiting root uptake and translocation.<sup>7,11,72–77</sup> In contrast, the nZVI + MT co-treatment further amplified the dominance of *Pseudomonadota* and enriched *Chloroflexota*, while reducing the abundance of *Actinomycetota*, *Euryarchaeota*, and *Acidobacteriota*, and modestly increasing *Cyanobacteriota* and *Bacteroidota*. This shift reflects a transition toward a microbiome with greater metabolic flexibility and responsiveness to chemical and hormonal cues, favoring plant-growth-promoting and stress-mitigating functions.

At the genus level, distinct microbial assemblages emerged under each treatment (Fig. 5c and d; Fig. S12 in Appendix A). The nZVI + MT combination enriched beneficial genera such as *Massilia*, *Bradyrhizobium*, and *Noviherbaspirillum*, while suppressing potential opportunists or less mutualistic taxa, including *Defluviococcus*, *Mycobacterium*, *Arthrobacter*, *Gaiella*, *Methyloceanibacter*, *Pseudolabrys*, and *Conexibacter*. By contrast, nZVI alone promoted *Defluviococcus*, *Mycobacterium*, *Gaiella*, *Methyloceanibacter*, *Noviherbaspirillum*, *Conexibacter*, and *Pseudolabrys*, while reducing *Massilia*, *Arthrobacter*, and *Bradyrhizobium*. The consistent enrichment of *Noviherbaspirillum* under both treatments highlights its adaptation to iron redox cycling and potential role in plant–microbe hormonal crosstalk. *Massilia*, a well-documented plant growth-promoting rhizobacterium with high metal tolerance, contributes to Cd immobilization via EPS-mediated extracellular sequestration.<sup>76,78,79</sup> *Bradyrhizobium* enhances nitrogen fixation and supports plant antioxidant systems, thereby stabilizing redox homeostasis under stress.<sup>76,78,79</sup>

Functional profiling further elucidated the mechanisms underlying Cd immobilization and Se enrichment (Fig. 5d). In nZVI-amended soils, the Fe(III)-reducing genus *Candidatus Acidoferrum* (Fig. S12) dominated the microbial community, indicating active iron cycling that drives iron (hydr)oxide plaque on roots and releases inorganic phosphate, both favoring Cd immobilization and plant growth.<sup>11,77</sup> Under the nZVI + MT treatment, *Sphingomonas* emerged as a key player,



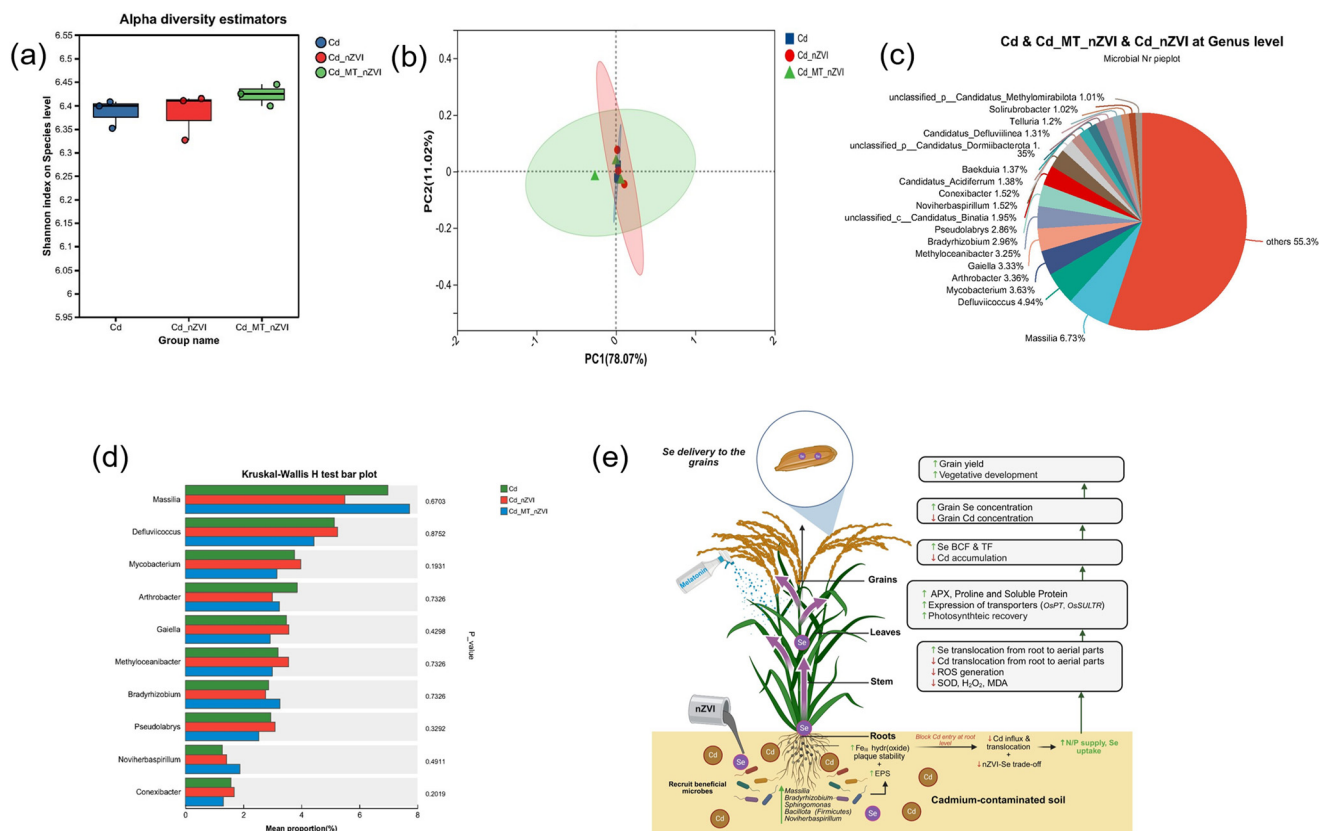


**Fig. 5** Effects of nZVI and MT on rhizosphere microbial dynamics. (a) Alpha-diversity (Simpson index), (b) principal coordinate analysis (PCoA), (c) genus-level community composition in Cd, Cd + nZVI, and Cd + MT + nZVI treatments, (d) Kruskal-Wallis *H* test bar plot comparing relative abundances among treatments, and (e) schematic model illustrating how nZVI and MT synergistically restructure the rhizosphere microbiome to reinforce Cd immobilization and enhance Se uptake and allocation. “Cd” = TF-Cd (Cd-only control); “Cd\_nZVI” = TF-Cd + nZVI (soil treated with 100 mg kg<sup>-1</sup> nZVI); “Cd\_MT\_nZVI” = T-Cd + MT + nZVI (MT at the T stage + nZVI soil amendment). EPS, exopolysaccharide production; BCF, bioconcentration factor; TF, translocation factor; SOD, superoxide dismutase; MDA, malondialdehyde.

known for its capacity for Cd biosorption, indole-3-acetic acid production, and phosphate solubilization, linking metal detoxification with phytohormone signaling and nutrient mobilization.<sup>12,76,80</sup> Together, the nZVI–MT co-treatment reconfigured the rhizosphere microbiome into a streamlined, functionally optimized consortium that directly supports host metal(loid) homeostasis (Fig. 5e). This engineered microbial community was enriched in key plant growth-promoting genera such as *Massilia*, *Bradyrhizobium*, and *Sphingomonas*, which collectively perform a suite of complementary and synergistic functions. These include the production of EPS and direct biosorption of Cd, thereby immobilizing the metal at the root–soil interface and reducing its bioavailability. Concurrently, nitrogen fixation and microbial-mediated antioxidants contribute to the stabilization of the plant’s redox status, while phosphate solubilization and phytohormone signaling enhance nutrient acquisition and systemic allocation, processes critical for Se uptake and long-distance translocation to grains. These findings are consistent with prior research demonstrating that the fungal endophyte *Beauveria bassiana* strain FE14 promotes growth of *Miscanthus floridulus* by reducing soil Cd bioavailability, modulating antioxidant enzyme activities, and reshaping root

endophytic bacterial networks, particularly enriching *Sphingomonas*, *Massilia*, and *Bradyrhizobium*.<sup>81</sup> The recurrence of these taxa across diverse plant–microbe–metal systems underscores their functional resilience and central role in integrated stress mitigation and growth promotion. In the present study, the enrichment of these beneficial genera aligns with observed plant-level outcomes, including reduced grain Cd BCF, elevated Se BCF and TF (section 3.2), and reduced ROS burden (section 3.3). In summary, by coupling nZVI-driven iron redox cycling and plaque formation with MT-mediated signaling that selectively enriched plant-growth-promoting rhizobacteria, the co-application established a microbiome that simultaneously achieve Cd restriction and Se enrichment, providing a robust microbial basis for the dual agronomic benefits.

## 4. Conclusion

Our findings demonstrate that stage-specific co-application of nZVI and MT effectively restricts Cd accumulation while enhancing Se enrichment in rice grown on contaminated soils. Evidence from physiological traits, redox homeostasis, transcriptomic profiles, and rhizosphere microbial analyses



indicates that this dual benefit arises from coordinated regulation at multiple biological levels. At the plant level, the treatment reduced Cd uptake and long-distance transport while reinforcing detoxification capacity and maintaining metabolic stability under stress. In parallel, Se acquisition and translocation were improved, thereby avoiding the micronutrient trade-offs typically associated with nZVI alone. At the rhizosphere level, microbial communities were restructured toward taxa that promote Cd immobilization, nutrient cycling, and stress alleviation, further supporting Se biofortification. Compared with single-agent applications, the stage-specific integration of nZVI and MT preserved the Cd-mitigating efficacy of nZVI while stabilizing redox balance and sustaining nutrient remobilization. These findings establish a mechanistically informed and agronomically viable strategy that synergistically integrates nanomaterial-enabled remediation with targeted phytohormonal regulation. This dual-pronged approach offers a sustainable pathway to cultivate rice with significantly reduced accumulation of toxic metals while simultaneously enhancing essential micronutrient profiles, thereby advancing both food safety and nutritional security in regions affected by heavy metal contamination. The stage-specific co-application of nZVI and MT is compatible with standard rice agronomy, demonstrates economic viability, and exhibits favorable environmental safety profiles, though scalability requires validation under diverse field conditions and advancement of regulatory frameworks for nanomaterials in agriculture.

## Author contributions

Saiqa Menhas: conceptualization, methodology, data curation, writing – original draft. Minjie Chen: data curation. Hui Jin: resources. Jiang Xu: resources. Saiyong Zhu: methodology. Muhammad Iqbal Zaman: writing – review & editing. Jie Hou: writing – review & editing, funding acquisition. Daohui Lin: conceptualization, writing – review & editing, supervision, funding acquisition.

## Conflicts of interest

The authors declare that they have no known competing financial interests or personal relationships that could have appeared to influence the work reported in this paper.

## Data availability

The data supporting this article have been included as part of the supplementary information (SI).

Supplementary information: SI associated with this article including experimental methods, result descriptions, 12 figures, and 1 table can be found in the online version. See DOI: <https://doi.org/10.1039/d5en00966a>.

## Acknowledgements

This work is supported by the National Natural Science Foundation of China (22494682, U21A20163, 22376181), the National Key Research and Development Program of China (2022YFC3702100), and the Key Research and Development Program of Zhejiang Province (2025C02215).

## References

- 1 S. Zhang, Y. Xu, M. Wu, X. Mao, Y. Yao, Q. Shen and M. Zhang, Geogenic enrichment of potentially toxic metals in agricultural soils derived from black shale in northwest Zhejiang, China: Pathways to and risks from associated crops, *Ecotoxicol. Environ. Saf.*, 2021, **215**, 112102.
- 2 J. Hu, G. Chen, K. Xu and J. Wang, Cadmium in Cereal Crops: Uptake and Transport Mechanisms and Minimizing Strategies, *J. Agric. Food Chem.*, 2022, **70**, 5961–5974.
- 3 F. Barman, T. Guha and R. Kundu, Exogenous Selenium Supplements Reduce Cadmium Accumulation and Restore Micronutrient Content in Rice Grains, *J. Soil Sci. Plant Nutr.*, 2025, **25**, 2275–2293.
- 4 H. Shang, C. Li, Z. Cai, Y. Hao, Y. Cao, W. Jia, L. Han, J. C. White, C. Ma and B. Xing, Biosynthesized Selenium Nanoparticles as an Effective Tool to Combat Soil Metal Stresses in Rice (*Oryza sativa* L.), *ACS Nano*, 2024, **18**, 19636–19648.
- 5 H. Zhang, S. Xie, N. Wan, B. Feng, Q. Wang, K. Huang, Y. Fang, Z. Bao and F. Xu, Iron plaque effects on selenium and cadmium stabilization in Cd-contaminated seleniferous rice seedlings, *Environ. Sci. Pollut. Res.*, 2023, **30**, 22772–22786.
- 6 R. Guo, R. Ren, L. Wang, Q. Zhi, T. Yu, Q. Hou and Z. Yang, Using machine learning to predict selenium and cadmium contents in rice grains from black shale-distributed farmland area, *Sci. Total Environ.*, 2024, **912**, 168802.
- 7 S. Zhu, M. Chen, H. Dai, T. Tian, W. Pan, J. Xu and D. Lin, Safe production of rice in Cd-polluted paddy fields by rhizosphere application of zero-valent iron nanoplates at specific growth stages, *Nano Today*, 2024, **56**, 102289.
- 8 S. Zhu, M. Chen, H. Dai, S. Menhas, J. Xu and D. Lin, Differential blocking effects of Fe<sup>0</sup> nanoplates on rice accumulation of typical essential and non-essential heavy metal elements in paddy fields, *Environ. Sci.: Nano*, 2024, **11**, 4151–4161.
- 9 T. Guha, A. Mukherjee and R. Kundu, Nano-Scale Zero Valent Iron (nZVI) Priming Enhances Yield, Alters Mineral Distribution and Grain Nutrient Content of *Oryza sativa* L. cv. Gobindobhog: A Field Study, *J. Plant Growth Regul.*, 2022, **41**, 710–733.
- 10 D. Hou, X. Cui, M. Liu, H. Qie, Y. Tang, R. Xu, P. Zhao, W. Leng, N. Luo, H. Luo, A. Lin, W. Wei, W. Yang and T. Zheng, The effects of iron-based nanomaterials (Fe NMs) on plants under stressful environments: Machine learning-assisted meta-analysis, *J. Environ. Manage.*, 2024, **354**, 120406.
- 11 Q. Bao, Y. Bao, J. Shi and Y. Sun, Nano zero-valent iron and melatonin synergistically alters uptake and translocation of



- Cd and As in soil-rice system and mechanism in soil chemistry and microbiology, *Environ. Int.*, 2024, **185**, 108550.
- 12 X. Cui, D. Hou, Y. Tang, M. Liu, H. Qie, T. Qian, R. Xu, A. Lin and X. Xu, Effects of the application of nanoscale zero-valent iron on plants: Meta analysis, mechanism, and prospects, *Sci. Total Environ.*, 2023, **900**, 165873.
  - 13 T. Guha, S. Barman, A. Mukherjee and R. Kundu, Nano-scale zero valent iron modulates Fe/Cd transporters and immobilizes soil Cd for production of Cd free rice, *Chemosphere*, 2020, **260**, 127533.
  - 14 P. G. P. S. Kulsum, R. Khanam, S. Das, A. K. Nayak, F. M. G. Tack, E. Meers, M. Vithanage, M. Shahid, A. Kumar, S. Chakraborty, T. Bhattacharya and J. K. Biswas, A state-of-the-art review on cadmium uptake, toxicity, and tolerance in rice: From physiological response to remediation process, *Environ. Res.*, 2023, **220**, 115098.
  - 15 G. Huang, D. Pan, M. Wang, S. Zhong, Y. Huang, F. Li, X. Li and B. Xing, Regulation of iron and cadmium uptake in rice roots by iron(iii) oxide nanoparticles: insights from iron plaque formation, gene expression, and nanoparticle accumulation, *Environ. Sci.: Nano*, 2022, **9**, 4093–4103.
  - 16 L. Ling, B. Pan and W.-x. Zhang, Removal of selenium from water with nanoscale zero-valent iron: Mechanisms of intraparticle reduction of Se(IV), *Water Res.*, 2015, **71**, 274–281.
  - 17 F. Chen, F. Jiang, M. K. Okla, Z. K. Abbas, S. M. Al-Qahtani, N. A. Al-Harbi, M. A. Abdel-Maksoud and L. M. Gomez-Olivan, Nanoparticles synergy: Enhancing wheat (*Triticum aestivum* L.) cadmium tolerance with iron oxide and selenium, *Sci. Total Environ.*, 2024, **915**, 169869.
  - 18 J. Wu, G. Huang, X. Cao, Y. Dai, L. Miao, J. Hou and B. Xing, Foliar Application of Reaction Products Derived from Selenite Removal by Iron Monosulfide for *Brassica rapa* ssp. *Chinensis* L, *Environ. Sci. Technol.*, 2022, **56**, 16281–16291.
  - 19 P. Zhou, P. Zhang, M. He, Y. Cao, M. Adeel, N. Shakoor, Y. Jiang, W. Zhao, Y. Li, M. Li, I. Azeem, L. Jia, Y. Rui, X. Ma and I. Lynch, Iron-based nanomaterials reduce cadmium toxicity in rice (*Oryza sativa* L.) by modulating phytohormones, phytochelatin, cadmium transport genes and iron plaque formation, *Environ. Pollut.*, 2023, **320**, 121063.
  - 20 C. Chang, H. Zhang, F. Huang and X. Feng, Understanding the translocation and bioaccumulation of cadmium in the Enshi seleniferous area, China: Possible impact by the interaction of Se and Cd, *Environ. Pollut.*, 2022, **300**, 118927.
  - 21 C. Zhou, L. Zhu, T. Zhao, R. A. Dahlgren and J. Xu, Fertilizer application alters cadmium and selenium bioavailability in soil-rice system with high geological background levels, *Environ. Pollut.*, 2024, **350**, 124033.
  - 22 E. Agathokleous, B. Zhou, J. Xu, A. Ioannou, Z. Feng, C. J. Saitanis, M. Frei, E. J. Calabrese and V. Fotopoulos, Exogenous application of melatonin to plants, algae, and harvested products to sustain agricultural productivity and enhance nutritional and nutraceutical value: A meta-analysis, *Environ. Res.*, 2021, **200**, 111746.
  - 23 M. A. Farooq, F. Islam, A. Ayyaz, W. Chen, Y. Noor, W. Hu, F. Hannan and W. Zhou, Mitigation effects of exogenous melatonin-selenium nanoparticles on arsenic-induced stress in *Brassica napus*, *Environ. Pollut.*, 2022, **292**, 118473.
  - 24 J. Huang, H. K. Jing, Y. Zhang, S. Y. Chen, H. Y. Wang, Y. Cao, Z. Zhang, Y. H. Lu, Q. S. Zheng, R. F. Shen and X. F. Zhu, Melatonin reduces cadmium accumulation via mediating the nitric oxide accumulation and increasing the cell wall fixation capacity of cadmium in rice, *J. Hazard. Mater.*, 2023, **445**, 130529.
  - 25 J. Wang, Y. Lu, S. Xing, J. Yang, L. Liu, K. Huang, D. Liang, H. Xia, X. Zhang, X. Lv and L. Lin, Transcriptome analysis reveals the promoting effects of exogenous melatonin on the selenium uptake in grape under selenium stress, *Front. Plant Sci.*, 2024, **15**, 1447451.
  - 26 S. Menhas, D. Lin, S. Zhu, S. Hayat, T. Aftab, W. Liu and K. Hayat, Melatonin as a multifaceted stress protector in rice: Mechanisms, synergies, and knowledge gaps, *J. Plant Physiol.*, 2025, **312**, 154577.
  - 27 M. Jiang, S. Dai, B. Wang, Z. Xie, J. Li, L. Wang, S. Li, Y. Tan, B. Tian, Q. Shu and J. Huang, Gold nanoparticles synthesized using melatonin suppress cadmium uptake and alleviate its toxicity in rice, *Environ. Sci.: Nano*, 2021, **8**, 1042–1056.
  - 28 R. Munir, M. U. Yasin, M. Afzal, M. Jan, S. Muhammad, N. Jan, C. Nana, F. Munir, H. Iqbal, F. Tawab and Y. Gan, Melatonin alleviated cadmium accumulation and toxicity by modulating phytohormonal balance and antioxidant metabolism in rice, *Chemosphere*, 2024, **346**, 140590.
  - 29 C. W. Qiu, M. Richmond, Y. Ma, S. Zhang, W. Liu, X. Feng, I. M. Ahmed and F. Wu, Melatonin enhances cadmium tolerance in rice via long non-coding RNA-mediated modulation of cell wall and photosynthesis, *J. Hazard. Mater.*, 2024, **465**, 133251.
  - 30 Z. Ulhassan, Q. Huang, R. A. Gill, S. Ali, T. M. Mwamba, B. Ali, F. Hina and W. Zhou, Protective mechanisms of melatonin against selenium toxicity in *Brassica napus*: insights into physiological traits, thiol biosynthesis and antioxidant machinery, *BMC Plant Biol.*, 2019, **19**, 507.
  - 31 Y. Q. Gao, R. Guo, H. Y. Wang, J. Y. Sun, C. Z. Chen, D. Hu, C. W. Zhong, M. M. Jiang, R. F. Shen, X. F. Zhu and J. Huang, Melatonin Increases Root Cell Wall Phosphorus Reutilization via an NO Dependent Pathway in Rice (*Oryza sativa*), *J. Pineal Res.*, 2024, **76**, e12995.
  - 32 M. K. Hasan, G. J. Ahammed, S. Sun, M. Li, H. Yin and J. Zhou, Melatonin Inhibits Cadmium Translocation and Enhances Plant Tolerance by Regulating Sulfur Uptake and Assimilation in *Solanum lycopersicum* L, *J. Agric. Food Chem.*, 2019, **67**, 10563–10576.
  - 33 M. Faisal, M. Faizan, S. Soysal and A. A. Alatar, Synergistic application of melatonin and silicon oxide nanoparticles modulates reactive oxygen species generation and the antioxidant defense system: a strategy for cadmium tolerance in rice, *Front. Plant Sci.*, 2024, **15**, 1484600.
  - 34 G. J. Ahammed, M. Wu, Y. Wang, Y. Yan, Q. Mao, J. Ren, R. Ma, A. Liu and S. Chen, Melatonin alleviates iron stress by



- improving iron homeostasis, antioxidant defense and secondary metabolism in cucumber, *Sci. Hortic.*, 2020, **265**, 109205.
- 35 S. Ali, B. Ali, I. A. Sajid, S. Ahmad, M. A. Yousaf, Z. Ulhassan, K. Zhang, S. Ali, W. Zhou and B. Mao, Synergistic effects of exogenous melatonin and zinc oxide nanoparticles in alleviating cobalt stress in *Brassica napus*: insights from stress-related markers and antioxidant machinery, *Environ. Sci.: Nano*, 2025, **12**, 368–387.
- 36 Q. Bao, W. Bao, Y. Li, S. Zhang, F. Lian and Y. Huang, Silicon combined with foliar melatonin for reducing the absorption and translocation of Cd and As by *Oryza sativa* L. in two contaminated soils, *J. Environ. Manage.*, 2021, **287**, 112343.
- 37 G. Su, B. Chen, X. Wu, J. Xu, K. Yang and D. Lin, nZVI decreases N<sub>2</sub>O emission from pesticide-contaminated paddy soil, *Sci. Total Environ.*, 2023, **892**, 164613.
- 38 S. Menhas, M. Chen, H. Jin, J. Xu, S. Zhu and D. Lin, Plant growth stage and melatonin concentration dependency together drive the metal-nutrient dynamics of rice in paddy soil, *Int. J. Phytorem.*, 2025, **27**, 958–971.
- 39 Y. Liu, T. Wu, J. C. White and D. Lin, A new strategy using nanoscale zero-valent iron to simultaneously promote remediation and safe crop production in contaminated soil, *Nat. Nanotechnol.*, 2021, **16**, 197–205.
- 40 S. Menhas, X. Yang, K. Hayat, J. Bundschuh, X. Chen, N. Hui, D. Zhang, S. Chu, Y. Zhou, E. F. Ali, M. Shahid, J. Rinklebe, S. S. Lee, S. M. Shaheen and P. Zhou, Pleiotropic melatonin-mediated responses on growth and cadmium phytoextraction of *Brassica napus*: A bioecological trial for enhancing phytoremediation of soil cadmium, *J. Hazard. Mater.*, 2023, **457**, 131862.
- 41 S. Menhas, X. Yang, K. Hayat, A. Ali, E. F. Ali, M. Shahid, S. M. Shaheen, J. Rinklebe, S. Hayat and P. Zhou, Melatonin enhanced oilseed rape growth and mitigated Cd stress risk: A novel trial for reducing Cd accumulation by bioenergy crops, *Environ. Pollut.*, 2022, **308**, 119642.
- 42 L. Lin, W. Zhou, H. Dai, F. Cao, G. Zhang and F. Wu, Selenium reduces cadmium uptake and mitigates cadmium toxicity in rice, *J. Hazard. Mater.*, 2012, **235–236**, 343–351.
- 43 D. Lei, H. Cao, K. Zhang, K. Mao, Y. Guo, J. H. Huang, G. Yang, H. Zhang and X. Feng, Coupling of different antioxidative systems in rice under the simultaneous influence of selenium and cadmium, *Environ. Pollut.*, 2023, **337**, 122526.
- 44 H. Yang, Y. Wu, J. Che, W. Wu, L. Lyu and W. Li, LC-MS and GC-MS Metabolomics Analyses Revealed That Different Exogenous Substances Improved the Quality of Blueberry Fruits under Soil Cadmium Toxicity, *J. Agric. Food Chem.*, 2024, **72**, 904–915.
- 45 Q. Chen, W.-b. Qi, R. J. Reiter, W. Wei and B.-m. Wang, Exogenously applied melatonin stimulates root growth and raises endogenous indoleacetic acid in roots of etiolated seedlings of *Brassica juncea*, *J. Plant Physiol.*, 2009, **166**, 324–328.
- 46 A. Anwar, Y. Wang, M. Chen, S. Zhang, J. Wang, Y. Feng, Y. Xue, M. Zhao, W. Su, R. Chen and S. Song, Zero-valent iron (nZVI) nanoparticles mediate SlERF1 expression to enhance cadmium stress tolerance in tomato, *J. Hazard. Mater.*, 2024, **468**, 133829.
- 47 H. Ullah, B. Chen, A. Rashid, R. Zhao, A. Shahab, G. Yu, M. H. Wong and S. Khan, A critical review on selenium removal capacity from water using emerging non-conventional biosorbents, *Environ. Pollut.*, 2023, **339**, 122644.
- 48 Y. Guo, K. Mao, H. Cao, W. Ali, D. Lei, D. Teng, C. Chang, X. Yang, Q. Yang, N. K. Niazi, X. Feng and H. Zhang, Exogenous selenium (cadmium) inhibits the absorption and transportation of cadmium (selenium) in rice, *Environ. Pollut.*, 2021, **268**, 115829.
- 49 L. Zhang and C. Chu, Selenium Uptake, Transport, Metabolism, Reutilization, and Biofortification in Rice, *Rice*, 2022, **15**, 30.
- 50 A. A. Shah, N. A. Yasin, M. Mudassir, M. Ramzan, I. Hussain, M. H. Siddiqui, H. M. Ali, Z. Shabbir, A. Ali, S. Ahmed and R. Kumar, Iron oxide nanoparticles and selenium supplementation improve growth and photosynthesis by modulating antioxidant system and gene expression of chlorophyll synthase (CHLG) and protochlorophyllide oxidoreductase (POR) in arsenic-stressed *Cucumis melo*, *Environ. Pollut.*, 2022, **307**, 119413.
- 51 T. Bao, M. M. Damtie, C. Y. Wang, C. L. Li, Z. Chen, K. Cho, W. Wei, P. Yuan, R. L. Frost and B. J. Ni, Iron-containing nanominerals for sustainable phosphate management: A comprehensive review and future perspectives, *Sci. Total Environ.*, 2024, **926**, 172025.
- 52 Y. Huang, S. Peng, Y. Liu, G. Feng, Z. Ding, B. Xiang, L. Zheng, H. Cheng, S. Liu, H. Yao and J. Fang, Emerging Roles of Nanozymes in Plant and Environmental Sectors, *J. Agric. Food Chem.*, 2024, **72**, 23008–23023.
- 53 L. Huangfu, R. Chen, Y. Lu, E. Zhang, J. Miao, Z. Zuo, Y. Zhao, M. Zhu, Z. Zhang, P. Li, Y. Xu, Y. Yao, G. Liang, C. Xu, Y. Zhou and Z. Yang, OsCOMT, encoding a caffeic acid O-methyltransferase in melatonin biosynthesis, increases rice grain yield through dual regulation of leaf senescence and vascular development, *Plant Biotechnol. J.*, 2022, **20**, 1122–1139.
- 54 A. Banerjee, S. Samanta and A. Roychoudhury, Melatonin differentially refines the metabolome to improve seed formation during grain developmental stages and enhances yield in two contrasting rice cultivars, grown in arsenic-contaminated soil, *Plant Physiol. Biochem.*, 2024, **214**, 108849.
- 55 Z. Ulhassan, S. Ali, Z. Kaleem, H. Shahbaz, D. He, A. R. Khan, A. Salam, Y. Hamid, M. S. Sheteiwy, W. Zhou and Q. Huang, Effects of Nanosilica Priming on Rapeseed (*Brassica napus*) Tolerance to Cadmium and Arsenic Stress by Regulating Cellular Metabolism and Antioxidant Defense, *J. Agric. Food Chem.*, 2025, **73**, 4518–4533.
- 56 S. Ullah, M. I. Khan, M. N. Khan, U. Ali, B. Ali, R. Iqbal, Z. G. AR, B. M. AlMunqedhi, S. A. Razak, A. Kaplan, S. Ercisli and F. A. Soudy, Efficacy of Naphthyl Acetic Acid Foliar Spray in Moderating Drought Effects on the Morphological and Physiological Traits of Maize Plants (*Zea mays* L.), *ACS Omega*, 2023, **8**, 20488–20504.



- 57 S. Usman, A. A. Shah, M. Kaleem, Z. Noreen, W. Xu, E. A. Mahmoud and H. O. Elansary, Chitosan-Copper Nanocomposites Exterminate Cd Toxicity in L. through Improving Photosynthetic Attributes, Antioxidant Defense, and Reduced Cd Uptake, *ACS Omega*, 2025, **10**, 32879–32894.
- 58 Y. Weng, X. Bai, M. Kang, Y. Ji, H. Wang and Y. Liu, Detoxification Strategy of Titanium Oxide Nanoparticles Driving Endogenous Molecules Metabolism to Modulate Atrazine Conversion in *Lactuca sativa* L, *Environ. Sci. Technol.*, 2025, **59**, 6440–6451.
- 59 R. Xiong, W. Yu, J. Ma, X. Zheng, M. Tan, B. Chen and C. Chu, Reduction Potential Governs the Capacity of Quinones for Long-Distance Electron Transfer and Remote H(2)O(2) Generation, *Environ. Sci. Technol.*, 2025, **59**, 14465–14474.
- 60 Z. Xu, T. Zhang, Z. Xu, Y. Ma, Z. Niu, J. Chen, M. Zhang and F. Shi, Research Progress and Prospects of Nanozymes in Alleviating Abiotic Stress of Crops, *J. Agric. Food Chem.*, 2025, **73**, 8694–8714.
- 61 A. de Marcos Lapaz, C. H. P. Yoshida, J. G. Vieira, J. N. B. Silva, M. Dal-Bianco and C. Ribeiro, Promising role of selenium in mitigating the negative effects of iron deficiency in soybean leaves, *Environ. Exp. Bot.*, 2023, **211**, 105356.
- 62 M. A. Farooq, F. Hannan, F. Islam, A. Ayyaz, N. Zhang, W. Chen, K. Zhang, Q. Huang, L. Xu and W. Zhou, The potential of nanomaterials for sustainable modern agriculture: present findings and future perspectives, *Environ. Sci.: Nano*, 2022, **9**, 1926–1951.
- 63 H. Yang, H. Yu, S. Wang, H. Huang, D. Ye, X. Zhang, T. Liu, Y. Wang, Z. Zheng and T. Li, Comparative transcriptomics reveals the key pathways and genes of cadmium accumulation in the high cadmium-accumulating rice (*Oryza Sativa* L.) line, *Environ. Int.*, 2024, **193**, 109113.
- 64 P. Su, H. Kang, Q. Peng, W. A. Wicaksono, G. Berg, Z. Liu, J. Ma, D. Zhang, T. Cernava and Y. Liu, Microbiome homeostasis on rice leaves is regulated by a precursor molecule of lignin biosynthesis, *Nat. Commun.*, 2024, **15**, 23.
- 65 J. Gago, M. Nadal, M. J. Clemente-Moreno, C. M. Figueroa, D. B. Medeiros, N. Cubo-Ribas, L. A. Cavieres, J. Guliás, A. R. Fernie, J. Flexas and L. A. Bravo, Nutrient availability regulates *Deschampsia antarctica* photosynthetic and stress tolerance performance in Antarctica, *J. Exp. Bot.*, 2023, **74**, 2620–2637.
- 66 K. Li, J. Li, F. Qin, H. Dong, W. Wang, H. Luo, D. Qin, C. Zhang and H. Tan, Nano zero valent iron in the 21st century: A data-driven visualization and analysis of research topics and trends, *J. Cleaner Prod.*, 2023, **415**, 137812.
- 67 J. Wang, Z. Fang, W. Cheng, X. Yan, P. E. Tsang and D. Zhao, Higher concentrations of nanoscale zero-valent iron (nZVI) in soil induced rice chlorosis due to inhibited active iron transportation, *Environ. Pollut.*, 2016, **210**, 338–345.
- 68 W. Zhao, Z. Wu, M. Amde, G. Zhu, Y. Wei, P. Zhou, Q. Zhang, M. Song, Z. Tan, P. Zhang, Y. Rui and I. Lynch, Nanoenabled Enhancement of Plant Tolerance to Heat and Drought Stress on Molecular Response, *J. Agric. Food Chem.*, 2023, **71**, 20405–20418.
- 69 M. A. Altaf, Y. Hao, H. Shu, M. A. Mumtaz, S. Cheng, M. N. Alyemeni, P. Ahmad and Z. Wang, Melatonin enhanced the heavy metal-stress tolerance of pepper by mitigating the oxidative damage and reducing the heavy metal accumulation, *J. Hazard. Mater.*, 2023, **454**, 131468.
- 70 A. K. Kathirvel, K. M. Karuppasami, V. Dhashnamurthi, G. Vellingiri, R. Muthurajan, A. Venugopal, A. Kuppasamy and S. Alagarsamy, Enhancement of grain yield in rice under combined drought and high-temperature stress conditions by maintaining photosynthesis through antioxidant enzyme activities by melatonin, *Plant Physiol. Rep.*, 2024, **29**, 262–277.
- 71 Q. Chen, L. Yu, W. Chao, J. Xiang, X. Yang, J. Ye, X. Liao, X. Zhou, S. Rao, S. Cheng, X. Cong, B. Xiao and F. Xu, Comparative physiological and transcriptome analysis reveals the potential mechanism of selenium accumulation and tolerance to selenate toxicity of *Broussonetia papyrifera*, *Tree Physiol.*, 2022, **42**, 2578–2595.
- 72 M. A. Halim, M. M. Rahman, M. Megharaj and R. Naidu, Cadmium Immobilization in the Rhizosphere and Plant Cellular Detoxification: Role of Plant-Growth-Promoting Rhizobacteria as a Sustainable Solution, *J. Agric. Food Chem.*, 2020, **68**, 13497–13529.
- 73 Y. Liu, Y. Wang, T. Wu, J. Xu and D. Lin, Synergistic Effect of Soil Organic Matter and Nanoscale Zero-Valent Iron on Biodechlorination, *Environ. Sci. Technol.*, 2022, **56**, 4915–4925.
- 74 L. Tian, J. Shen, G. Sun, B. Wang, R. Ji and L. Zhao, Foliar Application of SiO(2) Nanoparticles Alters Soil Metabolite Profiles and Microbial Community Composition in the Pakchoi (*Brassica chinensis* L.) Rhizosphere Grown in Contaminated Mine Soil, *Environ. Sci. Technol.*, 2020, **54**, 13137–13146.
- 75 T. Zheng, J. Hou, T. Wu, H. Jin, Y. Dai, J. Xu, K. Yang and D. Lin, Ferric Oxide Nanomaterials and Plant-Rhizobacteria Symbionts Cogenerate Iron Plaque for Removing Highly Chlorinated Contaminants in Dryland Soils, *Environ. Sci. Technol.*, 2024, **58**, 11063–11073.
- 76 A. P. Madigan, E. Egidi, F. Bedon, A. E. Franks and K. M. Plummer, Bacterial and Fungal Communities Are Differentially Modified by Melatonin in Agricultural Soils Under Abiotic Stress, *Front. Microbiol.*, 2019, **10**, 2616.
- 77 M. Liu, J. Wang, M. Xu, S. Tang, J. Zhou, W. Pan, Q. Ma and L. Wu, Nano zero-valent iron-induced changes in soil iron species and soil bacterial communities contribute to the fate of Cd, *J. Hazard. Mater.*, 2022, **424**, 127343.
- 78 M. Jiang, Y. Song, R. Yang, C. Zheng, Y. Zheng, H. Zhang, S. Li, Y. Tan, J. Huang, Q. Shu and R. Li, Melatonin activates the OsbZIP79-OsABI5 module that orchestrates nitrogen and ROS homeostasis to alleviate nitrogen-limitation stress in rice, *Plant Commun.*, 2023, **4**, 100674.
- 79 M. Jiang, F. Ye, F. Liu, M. Brestic and X. Li, Rhizosphere melatonin application reprograms nitrogen-cycling related microorganisms to modulate low temperature response in barley, *Front. Plant Sci.*, 2022, **13**, 998861.



- 80 J. Liu, J. Wang, T. Zhang, M. Li, H. Yan, Q. Liu, Y. Wei, X. Ji and Q. Zhao, Exogenous Melatonin Positively Regulates Rice Root Growth through Promoting the Antioxidant System and Mediating the Auxin Signaling under Root-Zone Hypoxia Stress, *Agronomy*, 2023, **13**, 386.
- 81 Y. Wang, S. Xiang, R. Chen, L. Chen, W. Lan, J. Fang and Y. Xiao, Enhancing *Miscanthus floridulus* remediation of soil cadmium using *Beauveria bassiana* FE14: Plant growth promotion and microbial interactions, *Ecotoxicol. Environ. Saf.*, 2025, **290**, 117745.

